PROPERTIES OF PHOTON DENSITY WAVES AT BOUNDARIES

L.O.Svaasand[#], D. Haskell[¤], B.Tromberg[&], and M. McAdams[¤]
[#]Norwegian Institute of Technology, Norway
[¤]Harvey Mudd College, Clairmont
[&]Beckman Laser Institute, University of California, Irvine

ABSTRACT

Optical techniques represent a valuable tool for analysis of turbid media. Recent development has emphasized dynamic measurements where either ultrashort laser pulses or high frequency amplitude modulated laser light are launched into the medium.[1-5] The properties of the transmitted light range from quasi-coherent in media with limited scattering to the almost randomized incoherent behavior in strongly turbid media. The present discussion considers the influence of a boundary between a heavily scattering medium with an almost isotropic diffuse light distribution and a non-scattering medium. This case can be approximated in terms of well established solutions of the diffusion equation.[6-7] It will further be demonstrated that the somewhat composite mathematical expressions can be interpreted in a very simple, intuitive manner. This type of approximation is, of course, of limited validity in the surface layer itself. However, the simplicity of this approximation might make it a valuable tool for several applications.

INTRODUCTION

The optical fluence rate, φ , can be expressed in terms of the solutions of a time dependent diffusion equation of the form,[4)]

$$X\nabla^2\varphi - \frac{\partial\varphi}{\partial t} - \frac{\varphi}{\tau} = -qc \tag{1}$$

where t is the time and q is the rate of generation of diffusely propagating photons per unit volume. The parameters c, X and τ are, respectively, the velocity of light in the medium, the optical diffusivity and the optical loss relaxation time. The last two parameters can also be expressed in terms of the optical scattering and absorption coefficients,

$$X = \frac{c}{3\left[\sigma(1-g)+\beta\right]} = \frac{c}{3\left[\sigma_{eff}+\beta\right]} \approx \frac{c}{3\sigma_{eff}}$$
$$\tau = \frac{1}{c\beta} \tag{2}$$

where σ, g , and $\sigma_{eff}=\sigma(1-g)$ are, respectively, the scattering coefficient, the average cosine of the scattering angle and the effective scattering

0-8194-1115-9/93/$6.00

coefficient. The optical absorption coefficient is given by β.
The net flux of the diffusely propagating photons can be expressed,

$$\vec{j} = -\frac{\mathrm{X}}{c} grad\varphi \tag{3}$$

where $\vec{j}$ is the flux vector.

ONE-DIMENSIONAL MODEL

The time and space dependence of a one-dimensional problem can easily be found by expressing the temporal behavior by its Laplace transform together with a spatial dependence of the form,

$$\mathcal{L}[\varphi(x,t)] = \varphi(x,s) \propto e^{-kx} \tag{4}$$

where k is a function of the Laplace parameter s. The value of k follows from the Laplace transform of the homogeneous form of Eq.1,

$$\varphi(x,s)\,[\mathrm{X}k^2 - s - \frac{1}{\tau}] = 0 \tag{5}$$

i.e., k is given by,

$$k = \pm\sqrt{\frac{1}{\mathrm{X}}(s + \frac{1}{\tau})} \tag{6}$$

When a finite amount, Q, of diffuse optical energy density is released per unit area of a planar layer at position x=α at time t=0, the flow of diffuse optical energy from the layer can be expressed from Eq.3,

$$-\mathrm{X}\frac{\partial}{\partial x}\varphi(x,s)\,|_{x=\alpha+} + \mathrm{X}\frac{\partial}{\partial x}\varphi(x,s)\,|_{x=\alpha-} = cQ \tag{7}$$

The corresponding boundary conditions in the surface layer at position x=0 can be expressed,

$$\mathrm{X}\frac{\partial}{\partial x}\varphi(x,s)\,|_{x=0+} = Ac\varphi(x,s)\,|_{x=0-} \tag{8}$$

where A is a photon flux transfer coefficient at the surface. This coefficient is dependent on the scattering and absorption properties of the medium and on the difference in index of refraction between the scattering medium and the adjacent non-scattering medium.

The solutions given by Eq.4 can be expressed in the form,

$$
\begin{gathered}
0<x<\alpha: \\
\varphi(x,s)=A_1 e^{kx}+A_2 e^{-kx} \\
\\
x>\alpha: \\
\varphi(x,s)=A_3 e^{-kx}
\end{gathered}
\tag{9}
$$

where k is the positive root of Eq.6.

The coefficients A_1, A_2 and A_3 follow from substitution of Eq.9 in the boundary conditions given by Eqs.7 and 8,

$$
\begin{gathered}
A_1=\frac{cQ}{2k\mathbf{X}}e^{-k\alpha} \\
\\
A_2=\frac{cQ}{2k\mathbf{X}}\frac{k\mathbf{X}-Ac}{k\mathbf{X}+Ac}e^{-k\alpha} \\
\\
A_3=\frac{cQ}{2k\mathbf{X}}\left(e^{k\alpha}+\frac{k\mathbf{X}-\alpha c}{k\mathbf{X}+Ac}e^{-k\alpha}\right)
\end{gathered}
\tag{10}
$$

The Laplace transform of the fluence rate can thus be expressed,

$$
\varphi(x,s)=\frac{cQ}{2\mathbf{X}}\left[\frac{1}{k}e^{-k|\alpha-x|}+\frac{1}{k}e^{-k(\alpha+x)}-2\frac{Ac}{\mathbf{X}}\left(\frac{1}{k(k+\frac{Ac}{\mathbf{X}})}e^{-k(\alpha+x)}\right)\right]
\tag{11}
$$

The time dependent solution follows from the inverse Laplace transform,

$$
\begin{gathered}
\varphi(x,t)=\mathcal{L}^{-1}\varphi(x,s)=cQ\Bigg[\frac{1}{2\sqrt{\pi\mathbf{X}t}}\left(e^{-\frac{(x-\alpha)^2}{4\mathbf{X}t}}+e^{-\frac{(x+\alpha)^2}{4\mathbf{X}t}}\right) \\
-\frac{1}{\psi}e^{\frac{x+\alpha}{\psi}+\frac{\mathbf{X}t}{\psi^2}}erfc\left(\frac{x+\alpha}{2\sqrt{\mathbf{X}t}}+\frac{\sqrt{\mathbf{X}t}}{\psi}\right)\Bigg]e^{-\frac{t}{\tau}}
\end{gathered}
\tag{12}
$$

where $\psi=\mathbf{X}/(Ac)$ has been substituted.

The photon flux transfer coefficient A can, as discussed above, be expressed in terms of the mismatch in index of refraction at the surface. The relation between the fluence rate, which is defined by the optical energy flux incident on an infinitesimal small sphere divided by the cross-sectional area of that sphere, and the radiance L, i.e. the energy flux in some direction per unit solid angle and unit area normal to that direction, is given by,

$$
\varphi=\int_{\Omega=0}^{4\pi}Ld\Omega
\tag{13}
$$

where the integral is taken over all solid angles Ω from 0 to 4π.

The radiance can be expressed by a series expansion in terms of a deviation from an isotropic distribution,

$$L = \frac{\varphi}{4\pi} + \frac{3}{4\pi}\vec{j}\cdot\vec{I} + \cdots \tag{14}$$

The first term on the right hand side expresses the completely isotropic distribution. The second term, which represents the contribution from a net vectorial flux $\vec{j}$ of diffusely propagating photons, gives the anisotropy in the direction given by the unit vector $\vec{I}$.

The irradiation, i.e. the radiant energy flux incident onto one side of a unit surface, will vary with orientation of the surface normal with respect to the direction of the flux. The maximum value will be obtained when the surface normal is antiparallel to $\vec{j}$, and the minimum value is obtained for the parallel orientation. These values are given by,

$$E = \int_0^{2\pi} \left[\frac{\varphi}{4\pi} + \frac{3}{4\pi}(\vec{j}\cdot\vec{I})\right](-\vec{n}\cdot\vec{I})\,d\Omega = \frac{\varphi}{4} \pm \frac{j}{2} \tag{15}$$

where E is the irradiance and $\vec{n}$ is the surface normal.

The Fresnel reflection at the tissue surface of light arriving from the interior of the tissue can be expressed,[11)]

$$\begin{aligned} E &= \int_0^{2\pi} \left[\frac{\varphi}{4\pi} + \frac{3}{4\pi}(\vec{j}\cdot\vec{I})\right] R(-\vec{n}\cdot\vec{I})\,d\Omega \\ &= R_\varphi \frac{\varphi}{4} + R_i \frac{j}{2} \end{aligned} \tag{16}$$

where R is the angular dependent Fresnel coefficient for the reflection of unpolarized light at an interface with a discontinuity in the index of refraction.[13)] The parameters R_ϕ and R_i, which are defined by the given integral, are the effective reflection coefficient for the fluence and for the flux, respectively. Equating the reflected light to the irradiation onto the tissue at the surface gives,(Eqs.15 and 16)

$$R_\varphi \frac{\varphi}{4} + R_j \frac{j}{2} = \frac{\varphi}{4} - \frac{j}{2} \tag{17}$$

The substitution of the boundary condition given in Eq.8 into this expression yields,

$$\varphi|_{x=0+} = -\frac{1+R_j}{1-R_\varphi}2j = -\frac{1+R_j}{1-R_\varphi}2\left(-\frac{X}{c}\frac{\partial}{\partial x}\varphi|_{x=0+}\right) = \frac{1+R_j}{1-R_\varphi}2A\varphi|_{x=0+} \tag{18}$$

The boundary parameter Ψ can thus be expressed,

$$\psi=\frac{\mathrm{X}}{Ac}=\frac{1+R_j}{1-R_\varphi}2\frac{\mathrm{X}}{c} \tag{19}$$

The diffusion theory is a priory not valid in the surface layer itself since the assumption of a quasi isotropic radiance has to be violated there. However, the results predicted by the diffusion theory in regions distance to the surface might still be very accurate.

The term in Eq.12 containing the complimentary error function can be written,[8-9]

$$-\frac{1}{\psi}e^{\frac{x+\alpha}{\psi}+\frac{\mathrm{X}t}{\chi^2}}erfc\left(\frac{x+\alpha}{2\sqrt{\mathrm{X}t}}+\frac{\sqrt{\mathrm{X}t}}{\psi}\right)= -\frac{1}{\psi\sqrt{\pi\mathrm{X}t}}\int_0^\infty e^{-\frac{\chi}{\psi}}e^{-\frac{(x+\alpha+\chi)^2}{4\mathrm{X}t}}d\chi \tag{20}$$

This relation enables a very simple characterization of the effect of the boundary; the presence of the boundary can be represented by a continuous distribution of planar image sinks extending from $x=-\alpha$ *to* $x=-\infty$ together with a localized planar image source of value +Q at position $x=-\alpha$. The sink is an exponentially decaying distribution with a relaxation length given by ψ,

$$Q\left(-\frac{2}{\psi}e^{-\frac{\chi}{\psi}}\right) \tag{21}$$

The total amount of the distributed sinks, which follows from the integral of this expression, is equal to -2Q. In the case of a totally reflecting surface the distance ψ becomes infinite large. The total image distribution then reduces to a single localized source, i.e., to the source of value +Q at position α above the surface.

This interpretation of the sink distribution also enables a very helpful simplification valid in regions distal to the surface. The influence of the surface can, for distances where $x>>\psi$, be approximated by two localized planar images: a source +Q at a distance equal to α above the surface together with sink -2Q at distance equal to $\alpha+\psi$. The separation between the image sink and the image source is thus proportional to the inverse value of the photon flux transfer coefficient A.

The complex amplitude of the fluence rate generated by a harmonically varying source of angular frequency ω can be expressed correspondingly from Eq.11 or from Eqs.12 and 20,

$$\varphi(x,\omega)=\frac{cI_\omega}{2\mathbf{X}k}\left(e^{-k|x-\alpha|}+e^{-k(x+\alpha)}-\int_0^\infty\frac{2}{\psi}e^{-\frac{\chi}{\psi}}e^{-k(x+\alpha+\chi)}d\chi\right)$$
$$=\frac{cI_\omega}{2\mathbf{X}k}\left(e^{-k|x-\alpha|}+e^{-k(x+\alpha)}-\frac{2}{1+k\psi}e^{-k(\alpha+x)}\right) \tag{22}$$

where I_ω is the amplitude of power density of the source, i.e., power per unit area. The expression for the complex wavenumber k in this equation follows from the positive root of Eq.6 when $s=j\omega$ have been substituted in that expression, i.e.,

$$k=\sqrt{\frac{1}{\mathbf{X}}\left(j\omega+\frac{1}{\tau}\right)}=$$
$$\frac{1}{\sqrt{2\mathbf{X}\tau}}\sqrt{\sqrt{1+(\omega\tau)^2}+1}\;+\;j\frac{1}{\sqrt{2\mathbf{X}\tau}}\sqrt{\sqrt{1+(\omega\tau)^2}-1} \tag{23}$$

The phase velocity and the attenuation of these waves are given, respectively, by the ratio between the angular frequency and the imaginary part of the wavenumber and by the real part of the wavenumber. The phase velocity in the high frequency region, where the frequency is much higher than the inverse loss relaxation time, i.e. $\omega>>1/\tau$, is given by $v_{ph}=\sqrt{2\mathbf{X}\omega}$ and the corresponding attenuation coefficient is $k_r=\sqrt{\frac{\omega}{\mathbf{X}}}$. The high frequency waves are dispersive with a phase velocity and an attenuation proportional to the frequency. The corresponding values for the low frequency region, where $\omega<<1/\tau$, are, respectively, $v_{ph}=2\sqrt{\frac{\mathbf{X}}{\tau}}$ and $k_r=\frac{1}{\sqrt{\tau\mathbf{X}}}=\frac{1}{\delta}$. The waves in the low frequency region are dispersion-less and the optical penetration depth is equal to the penetration depth δ for the time independent case.

The attenuation per wavelength is an important parameter for all wave applications. This quantity is for diffusive waves given by,

$$2\pi\frac{k_r}{k_i}=2\pi\frac{\sqrt{\sqrt{1+(\omega\tau)^2}+1}}{\sqrt{\sqrt{1+(\omega\tau)}-1}} \tag{24}$$

The attenuation per wavelength is in the high frequency region thus constant and equal to 2π, i.e. 27 dB. The attenuation per wavelength in the low frequency is correspondingly given by $4\pi/(\omega\tau)$. It is important to note that although the attenuation per unit length always is lower in the low frequency region than in the high frequency region, the attenuation per unit wavelength is always larger in the low frequency region.

Tissue	Diffusivity X m^2/s	Relaxation time τ ps	Absorption coeff. β cm^{-1}	Scattering coeff. σ_{eff} cm^{-1}	Penetration depth δ mm	Phase velocity v_{ph} 1/c #
Bovine brain	64 000	424	0.11	11	5.2	0.12
Ocular sclera, human	26 500	583	0.08	25	3.9	0.06
Corpus callosum, human brain	14 300	583	0.08	50	2.9	0.05

Relative to velocity of light in a non-scattering medium with the same index of refraction. Index of refraction n=1.4; Wavelength 650 nm, Measured ex-vivo

Table 1. OPTICAL PROPERTIES OF TISSUES[12)]

The optical properties of some tissues are given in table 1. There are, however, only three independent set of parameters. When the index of refraction is given, the optical properties can be characterized either by the optical diffusivity and relaxation time (X,τ), by the effective scattering and absorption coefficient (σ_{eff},β), or finally by the optical penetration depth and low frequency phase velocity (δ,v_{ph}). The expressions for the boundary parameter Ψ for the various tissues in the case of index matched tissue surface and for the tissue/air interface are given in table 2.

Tissue	Diffusivity X m^2/s	Relaxation time τ ps	Index matched boundary $\frac{1+R_j}{1-R_\varphi}=1$ Ψ mm	Tissue/air interface $\frac{1+R_j}{1-R_\varphi}=2.95$ Ψ mm
Bovine brain	64 000	424	0.60	1.76
Ocular sclera, human	26 500	583	0.25	0.73
Corpus callosum, human brain	14 300	583	0.13	0.39

Table 2. BOUNDARY PARAMETERS

THREE-DIMENSIONAL MODEL

The solution of the three-dimensional problem can be formed in analogy with the one-dimensional problem. The fluence rate generated by the release of a Dirac δ-pulse of diffuse optical energy, Q_T, at some point in an infinite medium at time t=0 can be expressed by a Greens function of the form,[6,10]

$$\varphi(r,t)=\frac{cQ_T}{8\sqrt{(\pi\mathbf{X}t)^3}}e^{-\frac{r^2}{4\mathbf{X}t}} \tag{25}$$

where r is the distance from the source.

The presence of the boundary can, in the same manner as in the one-dimensional case, be represented by a sink/source image distribution. The images consist now of a continuous distribution of image sinks along the surface normal extending from $x=-\alpha$ *to* $x=-\infty$ together with a localized image point source of value $+Q_T$ at position $x=-\alpha$. The total amount of the distributed sinks is $-2Q_T$.

The distribution of light from an amount of optical energy, Q_T, released at time t=0 on the x-axis at a distance $x=\alpha$ from the surface can thus be expressed,

$$\varphi(r,t)=\frac{cQ_T}{8\sqrt{(\pi\mathbf{X}t)^3}}\left[e^{-\frac{(x-\alpha)^2}{4\mathbf{X}t}}+e^{-\frac{(x+\alpha)^2}{4\mathbf{X}t}}-\int_0^\infty\frac{2}{\psi}e^{-\frac{\chi}{\psi}}e^{-\frac{(x+\alpha+\chi)^2}{4\mathbf{X}t}}d\chi\right]e^{-\frac{\rho^2}{4\mathbf{X}t}}e^{-\frac{t}{\tau}} \tag{26}$$

where ρ is the radial distance from the x-axis.

The distribution of the sources is illustrated in Fig.1.

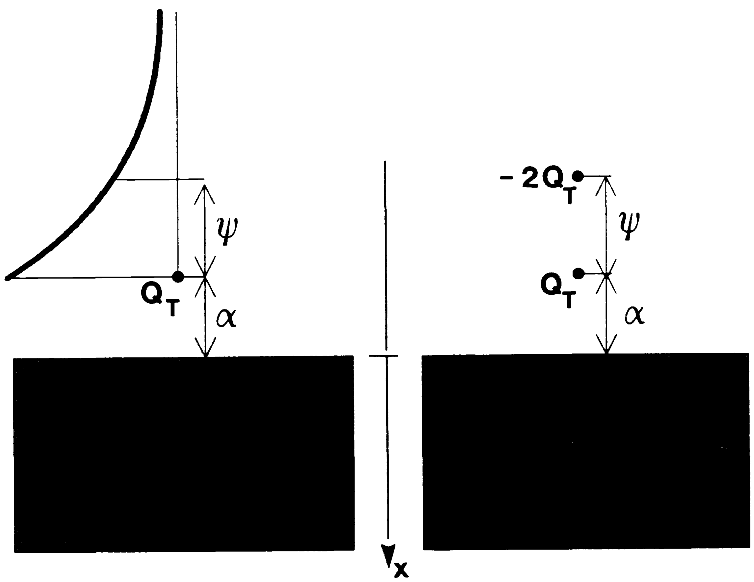

Fig.1. Source and image distribution in the case of a point source embedded in a turbid medium. Fig.1a (left hand side): exact image distribution. Fig.1b (right hand side): approximate distribution.

Figure 1a shows the primary point source in the turbid medium (hatched area) at distance $x=\alpha$ from the surface together with the images, i.e., the exponentially decaying sink distribution extending from $x=-\alpha$ together with the image point source at position $x=-\alpha$. The corresponding simplified image distribution for the calculation of the fluence rate in more distal regions is given in Fig.1b.

In the case of a totally reflecting surface the relaxation length ψ becomes infinite large. The total image distribution then reduces to a single localized source, i.e., to the image source of value $+Q_T$ at position α above the surface. In the case of a partially transmitting surface ψ is reduced in proportion to the inverse value of the transfer coefficient A, i.e., $\psi=X/(Ac)$. However, it should be borne in mind that the validity of diffusion model is reduced as the transmission through the surface approaches the totally transmitting case.

The calculated optical fluence rate from a δ-pulse of diffuse optical energy released at time t=0 at a depth of 1 mm below the surface in a bovine brain is shown in fig.2a. The figure shows the fluence rate at the surface, and the distance between the source and the detector fiber is 5 mm. The fluence rate is given by the vertical axis, and the left and right hand side horizontal axis give, respectively, the parameter ψ and the time t. The parameter Ψ varies from Ψ=0.60 mm to 10 mm corresponding to, respectively, a totally transmitting case with index matched boundary and to an almost totally reflective boundary. The time axes goes from t=0.2 ps to 100 ps. The calculation demonstrates that the velocity of the pulse envelope along the surface is faster in the totally transmitting case than in the almost totally reflecting case; loss of photons through the boundary results in a smaller but faster moving pulse envelope. The corresponding value for the fluence rate at a depth of 2 mm below the surface is shown in fig.2b. The influence due to the presence of the boundary is here significantly reduced.

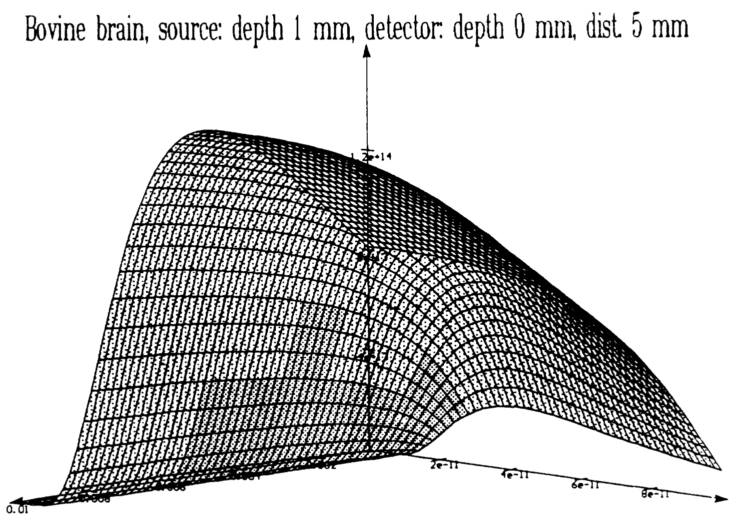

Figure 2a. Optical fluence rate in the surface layer of a bovine brain.

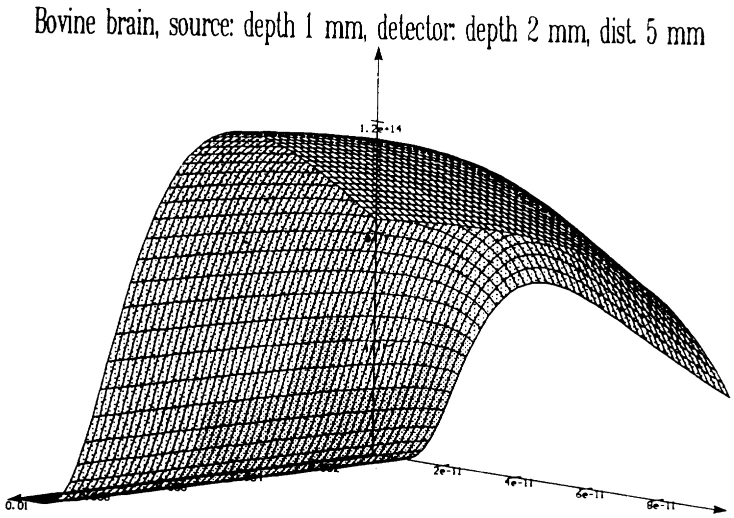

Figure 2b. Optical fluence rate at 2 mm depth below the surface of bovine brain.

The complex amplitude of the fluence rate generated by a harmonically varying source in an infinite large medium can be expressed,

$$\varphi(r,\omega)=\frac{cP_{\omega}}{4\pi \mathrm{X} r}e^{-kr} \tag{27}$$

where P_{ω} is the amplitude of the power of the source, r is the distance from the source and ω is the angular frequency. The complex wavenumber k is given by Eq.6.

The corresponding value for the fluence rate in a medium bounded by a planar surface is correspondingly,

$$\varphi(r,\omega)=\frac{cP_{\omega}}{4\pi \mathrm{X}}\Bigg(\frac{e^{-k\sqrt{(x-\alpha)^2+\rho^2}}}{\sqrt{(x-\alpha)^2+\rho^2}}+\frac{e^{-k\sqrt{(x+\alpha)^2+\rho^2}}}{\sqrt{(x+\alpha)^2+\rho^2}} - \int_0^{\infty}\frac{2}{\psi}e^{-\frac{\chi}{\psi}}\frac{e^{-k\sqrt{(x+\alpha+\chi)^2+\rho^2}}}{\sqrt{(x+\alpha+\chi)^2+\rho^2}}d\chi\Bigg) \tag{28}$$

The corresponding simplified image source distribution for calculation of the fluence rate in distal regions is here a point sink of value $-2P_{\omega}$ and at a point source $+P_{\omega}$ positioned, respectively, at $\alpha+\psi$ and at α above the surface. The fluence rate can then be approximated by,

$$\varphi(r,\omega)=\frac{c}{4\pi X}\sum_{n=1}^{n=3} q_n \frac{e^{-kr_n}}{r_n} \tag{28}$$

where $q_1=+P_\omega$, $q_2=+P_\omega$, $q_3=-2P_\omega$. The distances r_1, r_2 and r_3 are, respectively, the distance from the real source, the distance from the image source and the distance from the image sink.

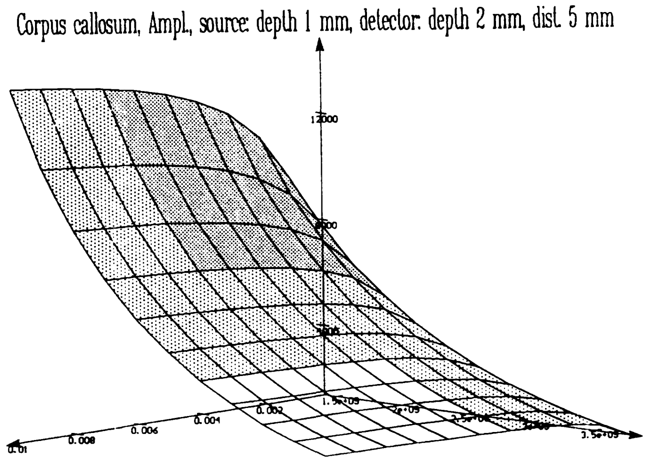

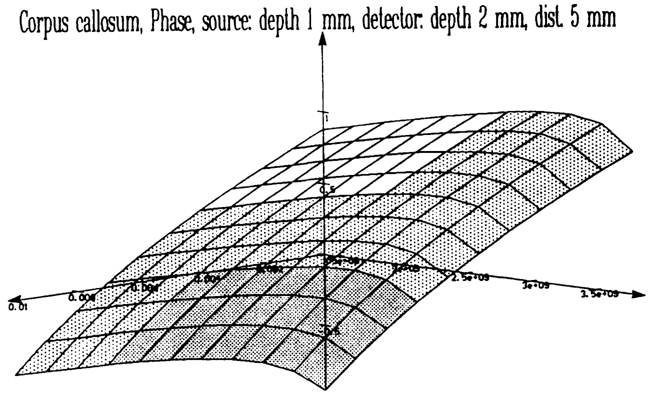

Figure 3. Optical fluence rate at 2 mm depth below the surface of corpus callosum of the human brain. Fig.3a (upper figure) shows the amplitude and fig.3b (lower figure) shows the phase.

The calculated optical fluence rate from an harmonically varying source of diffuse optical energy in corpus callosum of the human brain is shown in fig.3. The depth of the source is 1 mm and the figure shows the fluence rate at a depth of 2 mm, and the distance between the source and the detector fiber is 5 mm. The left and right hand side horizontal axis give, respectively, the parameter ψ and the frequency. The parameter Ψ varies from Ψ=0.13 mm to 10 mm corresponding to, respectively, a totally transmitting case with index matched boundary and to an almost totally reflective boundary. The frequency axes goes from f=1.5 GHz to 3.5 GHz. The amplitude is given by the vertical axis in fig.3a whereas the phase-shift in radians is given by the vertical axis in fig.3b. The reduced phase shift for the totally transmitting case indicates a higher phase velocity than in the almost totally reflecting case; loss of photons through the boundary results in a higher phase velocity. This loss of photons will equally result in a reduced amplitude as demonstrated in fig.3a. Figure 3a. also shows that the amplitude is reduced with increasing frequency, and fig.3b shows correspondingly that the phase velocity increases with increasing frequency.

ACKNOWLEDGEMENTS

This work was performed with support from The George Hewitt Foundation for Medical Research, the Office of Naval Research grant #N00014-91-C-0134, and the Department of Energy grant #DE-FG03-91 ER61227.

REFERENCES

1) Fishkin J, Gratton E, vandeVen M.J, Mantulin W.W. Diffusion of Intensity Modulated Near-Infrared Light in Turbid Media, SPIE Proceedings.1991; 1431:122-135.

2) Patterson M.S, Chance B., and Wilson B.C. Time-Resolved Reflectance and Transmittance for the Non-Invasive Measurements of Tissue Optical Properties. Applied Optics. 1989; 28:2331-2336.

3) Yoo K.M, Xing Q, Alfano R.R. Imaging Objects Hidden in Highly Scattering Media using Femtosecond Second-Harmonic-Generation Cross-Correlation Time Gating. Optics Letters. 1991; 16:1019-1021.

4) Svaasand L.O, Tromberg B.J. On the Properties of Optical Waves in Turbid Media. SPIE Proceedings. 1991; 1525:41-50.

5) Ishimaru A. Diffusion of Light in Turbid Materials, Appl.Optics. 1989; 28:2210-2215.

6) Carslaw H.S., Jaeger J.C. Conduction of Heat in Solid, Oxford at the Clarendon Press (1959)

7) Ben-Avraham D., Taitelbaum H., Weiss G.H. Boundary Conditions for a Model of Photon Migration in a Turbid Medium. Lasers in the Life Sciences. 1991; 4:29-36.

8) Bryan, Proc.Camb.Phil.Soc. 1891; 7:246

9) Carslaw H.S., Jaeger J.C. Conduction of Heat in Solid, Oxford at the Clarendon Press (1959) p.359

10) Ibid p.371.

11) Keijzer M., Star W.M., Storchi P.R.M. Optical Diffusion in Layered Media, Appl.Opt. 1988;27:1820-1824

12) Svaasand L.O., Tromberg B.J., Haskell R., Tsay T., Berns M.W. Tissue Characterization and Imaging Using Photon Density Waves, Optical Engineering Feb.1993 (in press)

13) Landau L.D., Lifshitz E.M. Electrodynamics of Continuous Media, Pergamon Press, Oxford (1960)